RSC Advances

ROYAL SOCIETY OF CHEMISTRY

www.rsc.org/advances

Aminoparticles – Synthesis, Characterisation and Application in Water Purification

Roshan Dsouza and Suresh Valiyaveettil*
Department of Chemistry, National University of Singapore
3 Science Drive 3, Singapore 117543
Email. chmsv@nus.edu.sg

Abstract

Polymer microparticles have been used in catalysis, sensing, environmental and biomedical applications. In this paper, synthesis and characterization of amine functionalized polymer microparticles or aminoparticles via copolymerisation of glycidyl methacrylate and styrene monomers are reported. The surface of microspheres was grafted with different amines – ethylenediamine, hexamethylenediamine, xylylenediamine and *n*-butylamine to increase the number and types of amino groups on the surface. The amine content on the microsphere surface was estimated and compared using elemental analyses and volumetric titration method. The fully characterized aminoparticles were used for the extraction of heavy metal ions and emerging pollutants such as gold and silver nanoparticles from aqueous solutions. The effect of contact time and concentrations of adsorbates on the extraction efficiency of pollutants, adsorption kinetics and isotherms were studied in detail. The extraction efficiencies of the synthesized particles were proportional to surface amine content and surface charges of the particles. Such particles will be useful towards developing novel column materials for analytical separations.

Keywords: Amine polymer, Microspheres, Adsorption, Nanoparticles

Introduction

Reactive polymers with amine functional groups have been used in a number of biomedical applications such as drug carriers,[1] biosensors,[2] coating materials for antifouling applications[3] and in electrochemical sensors.[4] In addition, amine groups can serve as functionalization sites for covalently attaching bioactive molecules[5] such as enzymes, peptides,[6] proteins,[7,8] and polysaccharides.[9] Recently, a series of amine functionalized particles and microgels were prepared and characterized, starting from vinylamine monomers.[10-13] Amine functionalised poly (glycidyl methacrylate) microparticles have been used for the synthesis of Au NPs,[14] in the diagnosis of cancer cells,[15] photocatalytic degradation studies,[16] recognition of albumin[17] and for environmental applications.[18-20]

Owing to the increased scarcity of potable water around the world, numerous simple methods have been developed and tested in recent years for water purification.[20-22] Pollutants such as heavy metal ions, dyes and metal nanoparticles in water induce adverse health effects on the ecosystem. Many recent studies have shown that both heavy metals[23-25] and metal nanomaterials[26-28] are toxic to living systems and it is essential to develop methodologies to eliminate them from water.

In this study, synthesis and characterisation of microparticles with primary and secondary amine groups on the surface are discussed and used them as potential adsorbents for the extraction of emerging pollutants such as metal nanoparticles from water (Figure 1).

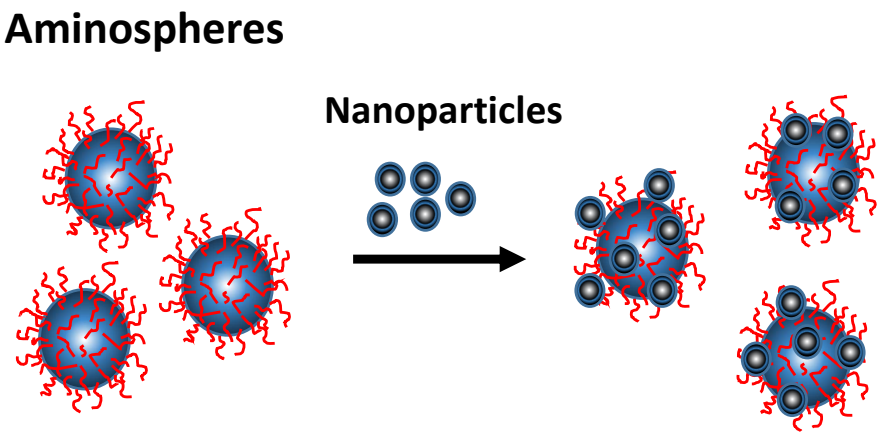

Figure 1. Schematic representation of adsorption of nanoparticles on the surface of aminoparticles.

Experimental

Materials

Glycidyl methacrylate (GMA), styrene, polyvinylpyrrolidone (PVP, Mw = 40 kDa), azobisisobutyronitrile (AIBN), ethylenediamine (EDA), hexamethylenediamine (HDA), *p*-xylylenediamine (XDA), *n*-butylamine (*n*-BA), silver nitrate ($AgNO_3$), potassium tetrachloroaurate trihydrate ($KAuCl_4 \cdot 3H_2O$), trisodium citrate dihydrate and sodium borohydride ($NaBH_4$) were purchased from Sigma Aldrich and used without further purification. Analytical grade ethanol was purchased from Fisher Scientific. Deionised water was used for all experiments. Stock solutions (1000 ppm) of $Cr_2O_7^{2-}$ and Pb^{2+} ions were prepared using potassium dichromate ($K_2Cr_2O_7$) and lead nitrate ($Pb(NO_3)_2$) salts.

Synthesis of Ag and Au nanoparticles

PVP and citrate capped gold (Au NPs) and silver (Ag NPs) nanoparticles were synthesized via reduction of $KAuCl_4 \bullet 3H_2O$ and $AgNO_3$ salts, respectively, using reported methods.[29,30] Aqueous solution of $AgNO_3$ (0.5 mL, 0.1 M) was diluted to 20 mL with deionised water. Trisodium citrate dihydrate (0.05 g, 0.17 mmol) dissolved in water (10 mL) was added dropwise and stirred for an hour. After diluting the mixture to 100 ml with deionised water, a freshly prepared solution of $NaBH_4$ (0.01 g, 0.26 mmol) dissolved in 10 mL water was added slowly and stirred for 24 h at room temperature. The resulting solution was centrifuged to get a solid pellet which was washed with water to remove unreacted starting materials. A similar procedure was employed in the preparation of PVP capped nanoparticles.

To prepare citrate capped gold nanoparticles (Au-Cit), trisodium citrate dihydrate (0.05 g, 0.017 mmol) was dissolved in 10 mL water and $KAuCl_4 \bullet 3H_2O$ (0.022 g, 0.05 mmol) in 50 mL water was added with stirring. Freshly prepared $NaBH_4$ solution (0.01 g, 0.26 mmol) dissolved in 10 mL water was added dropwise, diluted with water (130 mL) and stirred for 24 hr at room temperature and the obtained nanoparticles were purified to remove impurities. Purification was done by repeated centrifugation and washing with water, followed by testing the supernatant liquid for unreacted metal ions and capping agents. Similar procedure was followed for the synthesis of PVP-capped Au NPs with PVP (0.01 g in 10 mL water) was used as capping agents instead of citrate.

Both citrate and PVP capped Ag and Au NPs were characterised using transmission electron microscope (TEM), dynamic light scattering technique (DLS) and Zeta potential measurements to determine their size and surface charges. All data are summarized in Figure S1, S2 and Table S1 (ESI).

Synthesis of PGMA-*co*-PS microspheres by dispersion polymerisation

Synthesis of PGMA-*co*-PS microspheres was carried out using typical batch dispersion polymerisation procedure.[31] Glycidyl methacrylate (3.2 g) and PVP (0.3 g) dissolved in 18 mL of ethanol was purged with nitrogen for 30 minutes. Styrene (0.8 g) was added and the solution was heated to 75 °C and stirred for 20 h. After completion of the polymerisation, as monitored by GPC analyses, the particles were centrifuged, washed with ethanol and water several times to remove excess PVP and unreacted monomers. The isolated particles were dried under vacuum and used for further reaction after characterisation.

Functionalization of microparticles with amines

Amine groups were grafted onto the surface of PGMA-*co*-PS microspheres via ring opening reaction between amines and epoxy groups. Microspheres (0.5 g) were initially suspended in a 1:1 mixture of water and ethanol (10 mL). Ethylenediamine (EDA, 2 mL) was added to this dispersion and was stirred at 60 °C for 6 h.

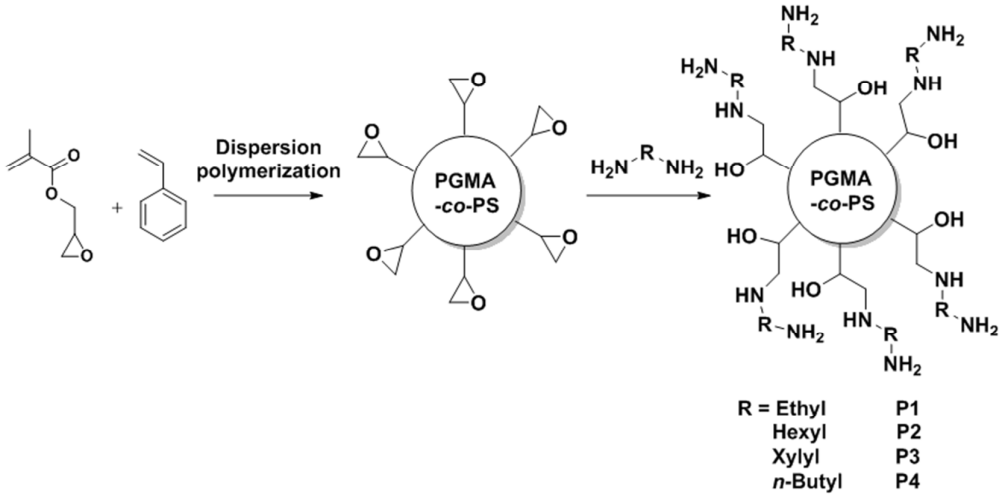

Scheme 1. General scheme showing the synthesis of amine functionalized microspheres

The amine substituted microparticles were centrifuged, washed several times with water, followed by ethanol and dried. Same procedure was followed for the synthesis of other amine

derivatives using hexamethylenediamine (HDA), xylenediamine (XDA) and *n*-butylamine (*n*-BA).

Characterization of aminoparticles

FT-IR measurements were used to determine the functional groups on microspheres and the spectra were recorded on a Bruker ALPHA FT-IR spectrophotometer with 4 cm^{-1} resolution in the spectral range of 500 - 4000 cm^{-1} using KBr as the matrix. The polymer microspheres were dissolved in appropriate solvents for further characterization. ^{1}H NMR spectrum of the precursor polymer (PGMA-*co*-PS) was recorded on Bruker Avance AV300 (300 MHz) instrument using $CDCl_3$ as solvent. Gel permeation chromatography (GPC) was performed on Waters e2695 alliance system equipped with Waters 2414 refractive index using THF as the eluent at a flow rate of 0.3 mL/min at 30 °C. Field emission scanning electron microscope (FE-SEM) images of the microspheres were recorded on a JEOL JSM-6701F instrument. The quantitative measurements of NPs during extraction experiments were performed using UV-Vis spectrophotometer (Shimadzu-1601) and the size was determined using a transmission electron microscope (TEM, JEOL JEM 2010). Dynamic light scattering (DLS) and zeta potential measurements were done using a Malvern Zetasizer Nano- ZS. The concentration of metal ions was quantitatively measured with Dual-view Optima 5300 DV Inductively coupled plasma - optical emission spectroscopy (ICP-OES) system.

The nitrogen content of the microspheres was determined using elemental analysis on Elementar Vario Micro Cube CHNS analyzer. Additionally, the concentration of amino groups on the microsphere surface was estimated by reported volumetric method.[32,33] Briefly, microspheres (20 mg) were added to dilute HCl solution (1 mM, 30 mL), sonicated for 30 min and shaken on a mechanical stirrer at ambient temperature. After 10 h, the microspheres were separated by centrifugation and the aqueous fraction was titrated against a 1 mM NaOH solution using phenolphthalein as indicator. The amine content of the microspheres was calculated using the equation:

$$\text{Amine concentration (mmol/g)} = (Co - Ce) \times 30 / 0.02 \qquad \text{Eqn (1)}$$

where, Co and Ce are the initial and steady state concentrations of HCl, respectively.

Extraction studies with nanoparticles and metal ions

Time-dependent extraction studies

The adsorption properties of amine functionalised microspheres were investigated by batch adsorption process. Microspheres (3 - 5 mg) were added to citrate or PVP-capped Au and Ag NP solutions (1.5 mL, 2.5 X 10^{-4} M) and placed on a mechanical stirrer for 3 h. All experiments were carried out at ambient temperature and neutral pH. At predetermined time intervals, the suspension was centrifuged at 5000 rpm and the microparticles were separated. The equilibrium concentrations of nanoparticles was analysed using UV absorption measurements.

To study the adsorption of metal ions in water, 5 mg of polymer particles were added to solutions of Pb^{2+} and $Cr_2O_7^{2-}$ ions and put on a mechanical stirrer at ambient conditions. The equilibrium concentrations of metal ions in solution were determined using ICP-OES analysis. The equilibrium adsorption capacities were calculated using the following equation:[34]

$$Q_e = \frac{(C_0 - C_e) \times V}{m} \qquad \text{(Eqn 2)}$$

where, C_o and C_e are the initial and equilibrium concentrations (in ppm), respectively of nanoparticles or metal ions, V is the volume of the solutions (mL) and *m* is the adsorbent dosage (mg).

Concentration dependent extraction studies

Suitable amounts of Ag NP and Au NP solutions (2.5 x 10^{-4} M) were diluted to obtain solutions with concentrations in the range of 5 - 50 ppm. Metal salt solutions with varying concentrations from 10 – 100 ppm were used for extractions. Aminoparticles (1.0 ± 0.1 mg) were dispersed in solution of nanoparticle or metal ions (2 mL) and kept on a shaker for 24 hours. Samples (1 mL) were collected, the solid was removed by centrifugation, and the extraction was quantified using UV-Vis spectroscopy for NPs and ICP analysis for metal ions.

Results and Discussion

Characterization of microspheres

In order to determine the constituents of the random copolymer formed by dispersion polymerisation method, the NMR spectrum of PGMA-*co*-PS microparticles was analysed in detail (Figure 2). The integral ratio of aromatic protons at (~ 7 ppm) to aliphatic –CH- (of GMA) at 4.3 ppm is 5:3 which suggests a styrene to GMA ratio of 1:3. The other peaks in the aliphatic region match with the polymeric structure.

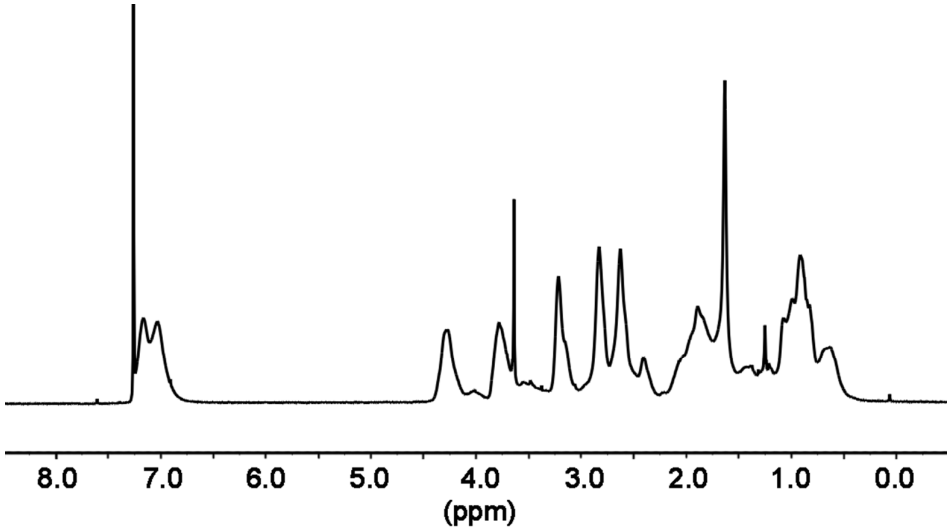

Figure 2. ^{1}H NMR spectrum of PGMA-*co*-PS microsphere dissolved and recorded in chloroform at ambient conditions.

GPC analysis of PGMA-*co*-PS polymers showed a number average molecular weight (Mn) of 39,010 with a broad PDI value of 2.45. These polymer microparticles with epoxide groups were used for surface functionalization with different amine substituents. Since the amine functionalised polymers were insoluble in common organic solvents, it was not possible to estimate the molecular weight by GPC. It is conceivable that the amine functionalization through nucleophilic attack on the epoxide ring does not alter the molecular weights or degradation of polymers significantly.

In order to characterize the surface amination process, FT-IR analyses were compared with starting PGMA-*co*-PS polymer. A comparison of the FT-IR spectra of precursor polymer PGMA-*co*-PS and amino polymers **P1** – **P4** are shown in Figure 3. In the spectrum of PGMA-*co*-PS, the strong peak at 1730 cm^{-1} corresponds to –C=O vibrations and the peaks at 1265 cm^{-1} and 995 cm^{-1} are assigned to the symmetrical and asymmetrical stretching frequencies of the epoxy group, respectively. During the subsequent amination reactions, the peak at 995 cm^{-1} disappeared owing to opening of epoxy ring and a new broad peak at 3400

cm^{-1} appeared due to the formation of –OH and -NH groups. A peak due to C-N bond stretching was seen at 1152 cm^{-1}. Aminoparticles prepared from all four diamines exhibited similar spectra owing to the similarities in the functional groups and polymer backbone.

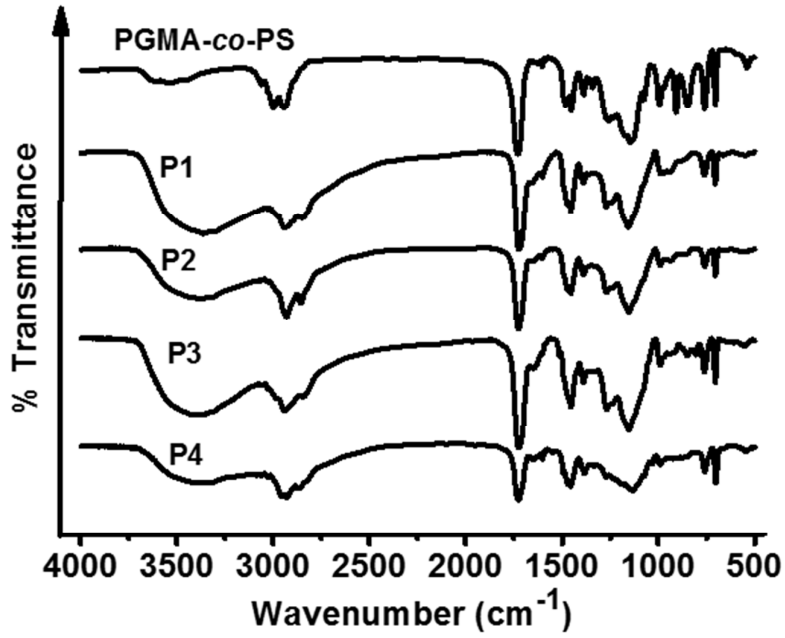

Figure 3. FT-IR spectra of PGMA-*co*-PS in comparison with aminoparticles **P1 – P4** on KBr matrix

The quantity of amine groups in aminoparticles was determined using elemental analyses and volumetric methods (Table 1). The elemental analyses confirm the N-atom content in the order of P1 > P2 > P4 > P3 and the amine concentration on the surface of the microspheres measured by volumetric method supports the same order.

Table 1. Elemental analyses, calculated N-content and surface zeta potential values of aminoparticles.

Microspheres	**C (%)**	**H (%)**	**N (%)**	**Amine content * (mmol/g)**	**Zeta potential (mV)**
PGMA-*co*-PS	63.1	8.18	<0.5	--	--
P1	55.13	7.45	8.07	4.53	+35.6
P2	60.02	7.92	5.74	4.04	+51.9
P3	62.60	7.51	4.38	3.34	+60.6

P4	62.37	8.41	4.25	2.69	+33.6

(As determined by volumetric method)*

Thermogravimetric analyses of aminoparticles

Thermogravimetric analysis (TGA) curves for microparticles were recorded using a heating rate of 10 °C/min (Figure S4). All particles exhibited similar TGA patterns with no significant weight loss below 200 °C under nitrogen atmosphere. The initial weight loss of 3-5% could be attributed to the loss of trapped moisture and solvents. The degradation occurred in a two-step process, one occurring between 200 to 380 °C and the second stage between 450 to 550 °C. The first stage of degradation can be attributed to the loss of alkyl groups along with decomposition of amine groups and the latter due to decomposition of polymer backbone.

Extraction Studies

Extraction of metal nanoparticles from aqueous solutions

Fully characterised aminoparticles were used for the extraction of citrate and PVP-stabilized Ag NPs and Au NPs from aqueous solutions. After extraction of the nanoparticles from water, the aminoparticles were separated using centrifugation (5000 rpm). The aqueous supernatant solution was analysed using UV-Vis spectroscopy to estimate the concentration of left over nanoparticles. The representative Uv-Vis spectra of metal nanoparticles before and after extraction are given in Figure S3 and data are tabulated in Table S2 (ESI).

Scanning electron microscopy was used for characterizing the morphology of the particles (Figure 4). The particles were mono-dispersed with an average diameter of 4 μm. The inherent roughness and presence of multiple amino groups on the surface of the polymer particles facilitated the removal of metal nanoparticles from aqueous solutions. The white spots observed on the surface of the aminoparticles after extraction in SEM micrographs (Figure 4) are confirmed as metal nanoparticles using EDX measurements.

In order to establish the role of surface amine groups, extraction of NPs using precursor polymer particles with no amine functional groups on the surface was performed. A known volume of metal NPs was added to a suspension of PGMA-*co*-PS particles in water and

stirred on a mechanical stirrer for 24 h. Polymer particles were separated by centrifugation at 5000 rpm and the supernatant solution was analysed using UV-Vis spectroscopy for the presence of metal NPs. From the absorbance data, it is evident that the polymer particles did not extract metal NPs due to the absence of amine groups on the surface. Additionally, there is a possibility that NPs may separate out from the solution during the centrifugation for separating the polymer particles. However, this was less likely owing to small size of NPs which require higher speeds (~ 20,000 rpm) and longer time to separate from solution. This was further checked and confirmed by centrifuging the NPs solution alone at lower speeds (less than 10,000 rpm) and no residue was collected.

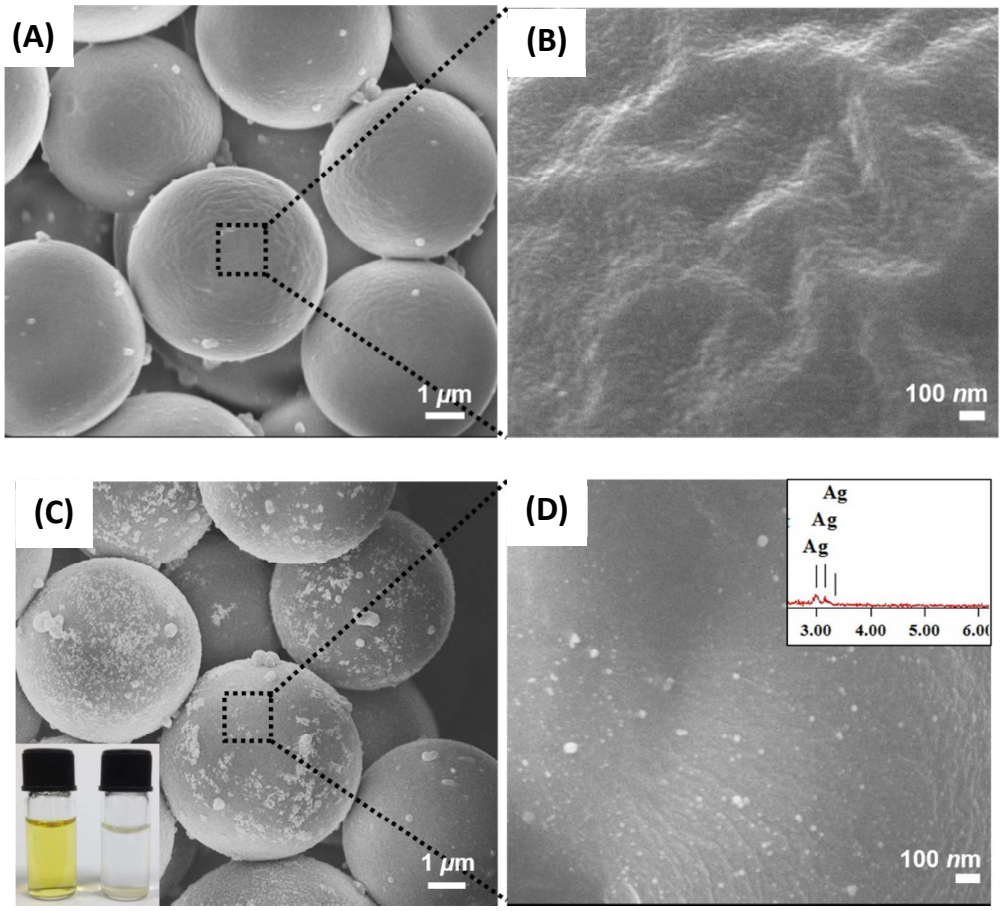

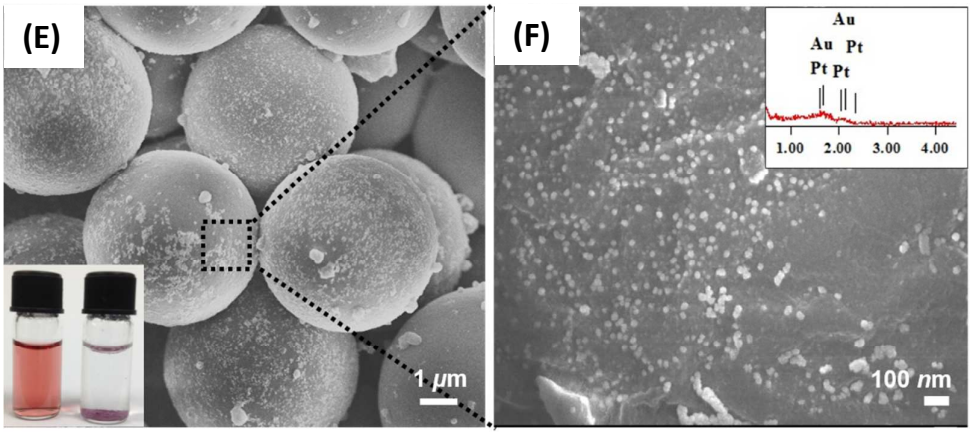

Figure 4. SEM spectra of **P1** before extraction (A and B) and after extraction of Ag-Cit (C and D) and Au-Cit NPs (E and F). Insets are the NP solutions before and after extraction of Ag-cit (C) and Au-cit NPs (E), respectively, and EDX spectra showing presence of NPs on the surface of aminoparticles.

Time dependent studies

Figure 5 shows the extraction efficiency of microspheres for citrate and PVP-coated Ag NPs and Au NPs as a function of time. The steady state was reached within a period of 15 - 20 min in the case of all nanoparticles. It is conceivable that the amine groups on the surface of microsphere influence the extraction of various pollutants from aqueous solutions. For all metal nanoparticles, the extraction efficiencies of microspheres is in the order P1 > P2 > P3 > P4. This is attributed to the small changes in the side group, which leads to changes in hydrophobicity/hydrophilicity and differences in type and structure of amine functional groups.

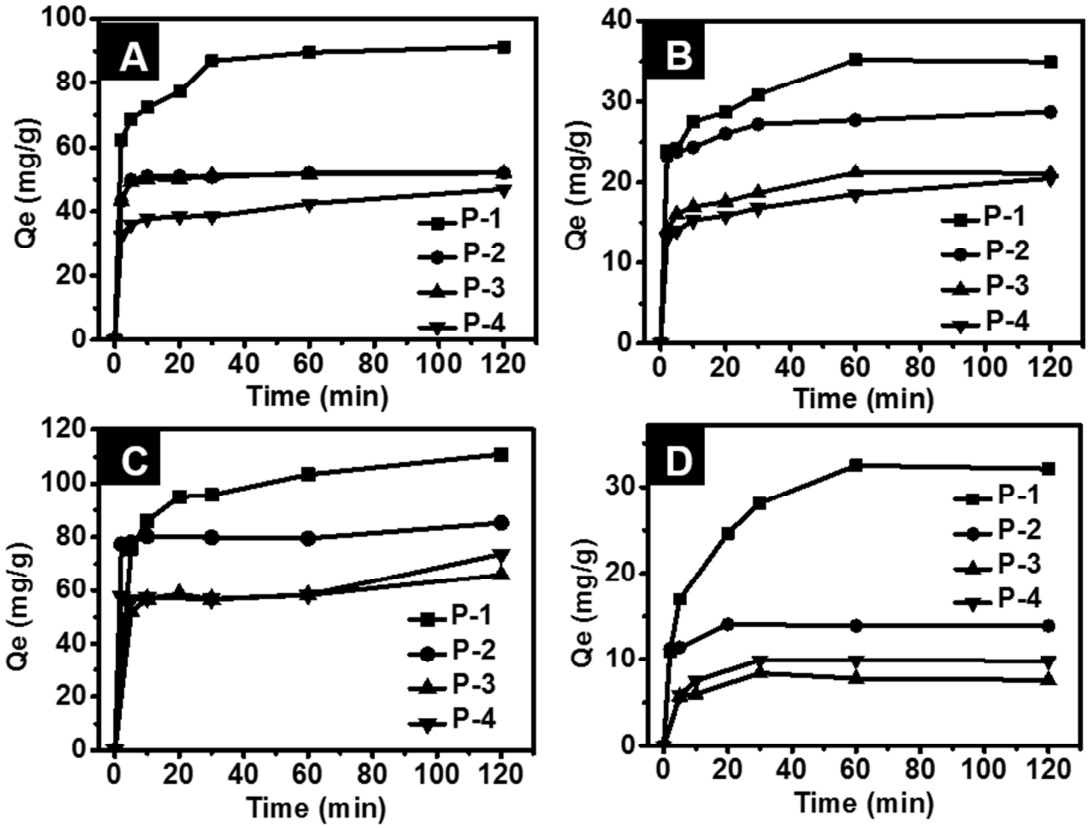

Figure 5. Effect of contact time on the adsorption efficiency of microparticles for the adsorption of (A) Ag-Cit, (B) Ag-PVP, (C) Au-Cit and (D) Au-PVP. (Nanoparticle concentration used in all cases is 2.5 X 10^{-4} M)

It is evident from the data that the extraction of citrate capped metallic NPs is significantly greater than the PVP-capped ones. The zeta-potential of citrate capped Ag and Au NPs are more negative (− 40.3 and − 37.3 mV, respectively, Refer Table S1) than PVP capped NP's (− 22.9 and − 21.4 mV, respectively) and hence are expected to interact strongly with positively charged amine functionalities on the surface of aminoparticles. The zeta potential of four aminoparticles are given in Table 1. The larger Q_e values of 91.3 (Ag-Cit) and 110.9 mg/g (Au-Cit) obtained for **P1** are higher than those reported in the literature for other common adsorbents.[35,36]

Adsorption kinetics

Understanding the adsorption kinetics provide information on the adsorption mechanism. Pseudo-first order and pseudo-second order models are the widely used models for studying the adsorption processes. The extraction of metal nanoparticles by the aminoparticles did not

follow the pseudo-first order kinetics. Hence the pseudo-second order model was used for data analysis. The equation is given in the linear form as:[37]

$$t/Q_t = t/Q_e + 1/(K_2.Q_e^2) \qquad \text{(Eqn 3)}$$

where K_2 (g mg^{-1} min^{-1}) is the pseudo-second order rate constant. The values of K_2 and Q_e were calculated from the slope and intercept of the *t/Q_t versus t* plots.

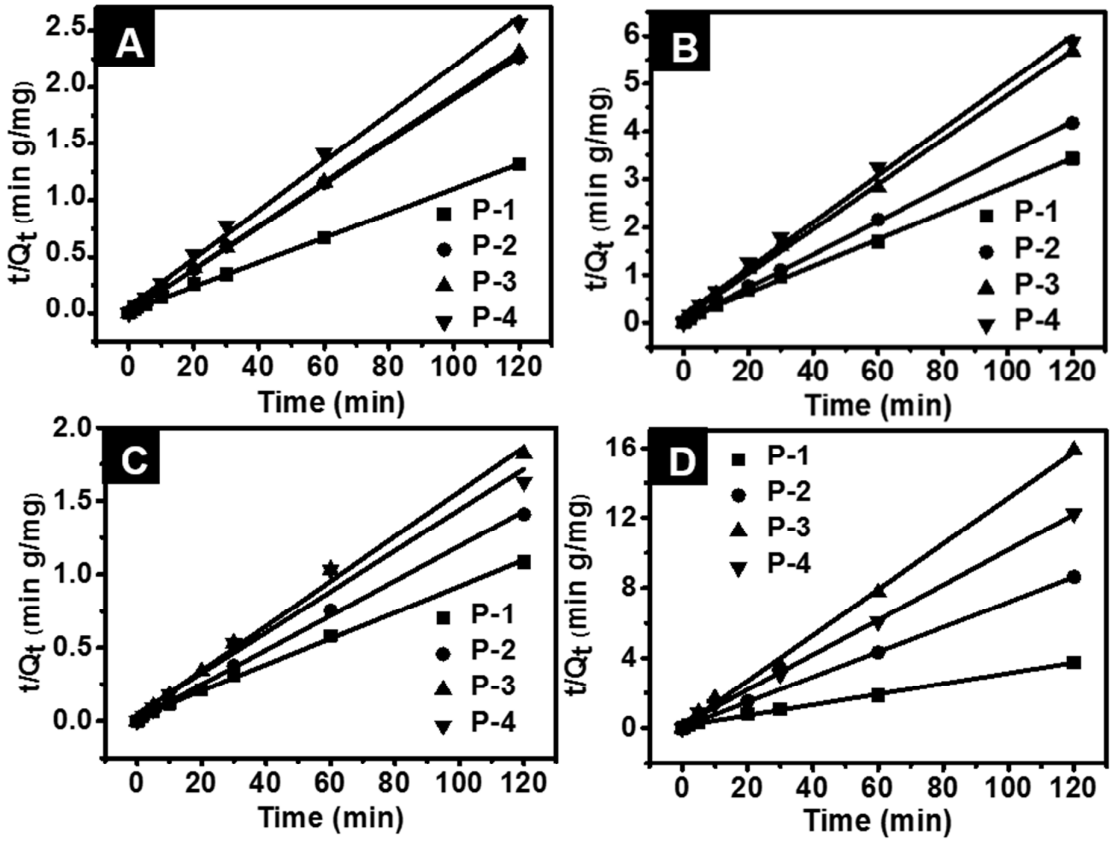

Figure 6. Pseudo-second order kinetics for the extraction of (A) Ag-Cit (B) Ag-PVP (C) Au-Cit and (D) Au-PVP using aminoparticles **P1 - P4**

Figure 6 shows the graphs of pseudo-second order model for NP adsorption. The ratio of the time and amount extracted is in linear relationship with time. The adsorption capacity, Q_e and the rate constant K_2 values were calculated from the slope and intercepts of the linear regression plots (Table 2). The correlation coefficients in all cases are closer to unity (R^2 ~ 0.99), which implies that the adsorption follows pseudo-second order model.

Table 2. Pseudo-second order constants and correlation coefficients for the extraction of NPs by aminoparticles **P1 – P4**

Nanoparticles	Amino-particles	Q_e(exp) (mg/g)	Pseudo-second order kinetic model		
			Q_e (mg/g)	K_2 (g/mg min)	R^2
Ag-Cit	**P1**	91.27	92.34	0.00598	0.999
	P2	51.27	52.99	0.03331	0.999
	P3	51.97	52.08	0.04915	0.999
	P4	46.91	46.95	0.00782	0.997
Ag-PVP	**P1**	34.97	35.59	0.01222	0.997
	P2	28.72	28.82	0.02787	0.999
	P3	21.11	21.46	0.02241	0.998
	P4	20.46	20.58	0.01458	0.994
Au-Cit	**P1**	110.88	111.98	0.00309	0.997
	P2	85.25	84.75	0.01379	0.999
	P3	65.89	65.57	0.00630	0.994
	P4	73.66	65.36	0.00502	0.98
Au-PVP	**P1**	32.11	33.33	0.00789	0.996
	P2	13.90	13.99	0.10651	0.999
	P3	8.35	7.65	0.25496	0.997
	P4	9.88	10.00	0.05785	0.998

Adsorption isotherms

Isotherms define the adsorption capacity at different concentrations of adsorbates. Two of the commonly used classic isotherm models - Langmuir and Freundlich - were selected to study the equilibrium adsorption.

In Langmuir isotherm model, the adsorption takes place at specific sites of adsorbent to form a monolayer on the surface. The Langmuir equation is expressed as,[37]

$$1/Q_e = 1/Q_m + 1/K_L Q_m C_e \qquad \text{(Eqn 4)}$$

where C_e is the initial adsorbate concentration (mg/L), Q_e is the amount adsorbed at equilibrium (mg/g), Q_m is the maximum adsorption capacity for the monolayer adsorption (mg/g) and K_L is Langmuir adsorption constant (L/g) which is related to the affinity of the

adsorbate on the binding sites. The values of Q_m ad K_L are calculated from the slopes and intercept values from the plots of $1/Q_e$ versus $1/C_e$.

On the other hand, the Freundlich isotherm predicts that the adsorption is not restricted to monolayer formation and can be reversible. The linear form of Freundlich adsorption isotherm is given as,[37]

$$\text{Ln } Q_e = 1/n \text{ Ln } C_e + \text{Ln } K_F \qquad \text{(Eqn 5)}$$

where K_F is the adsorption capacity at unit concentration and 1/n is the adsorption intensity explaining the strength of adsorption. The values can be calculated from the slopes and intercepts from the plots of *Ln Q_e versus Ln C_e*. The magnitude of 1/n determines the favourability of the adsorption.

Langmuir isotherm

Plots of *$1/Q_e$ vs $1/C_e$* for different nanoparticles (Figure 7) show a linear relationship suggesting the applicability of Langmuir model for data obtained for extraction studies. In addition, the favourability of the extractions can be predicted with a dimensionless constant, separation factor or equilibrium factor, given by the equation,

$$R_L = 1/(1+ K_L.C_0) \qquad \text{(Eqn 6)}$$

where, C_0 is the initial NP concentration (mg/L), $0 < R_L < 1$ indicates a favourable adsorption, while $R_L > 1$ indicates unfavourable adsorption. $R_L = 1$ corresponds to a linear adsorption process and $R_L = 0$ means an irreversible adsorption.

The Langmuir plots for the extraction of metal NPs by four aminoparticles are shown in Figure 7 and the corresponding Langmuir constants are depicted in Table 3. The correlation coefficients (R^2) for all microspheres is > 0.90 and are higher in values compared to the Freundlich isotherms. In addition, the calculated separation factor (R_L) values of 0.10 – 0.54 (Ag-Cit), 0.11 – 0.65 (Ag-PVP), 0.65 – 0.93 (Au-Cit) and 0.58 – 0.71 (Au-PVP) for initial NP concentrations of 5 – 50 ppm indicate a favourable adsorption as explained by Langmuir model. Also, hence the adsorption of metal NPs takes place at specific adsorption sites on the microsphere surface.

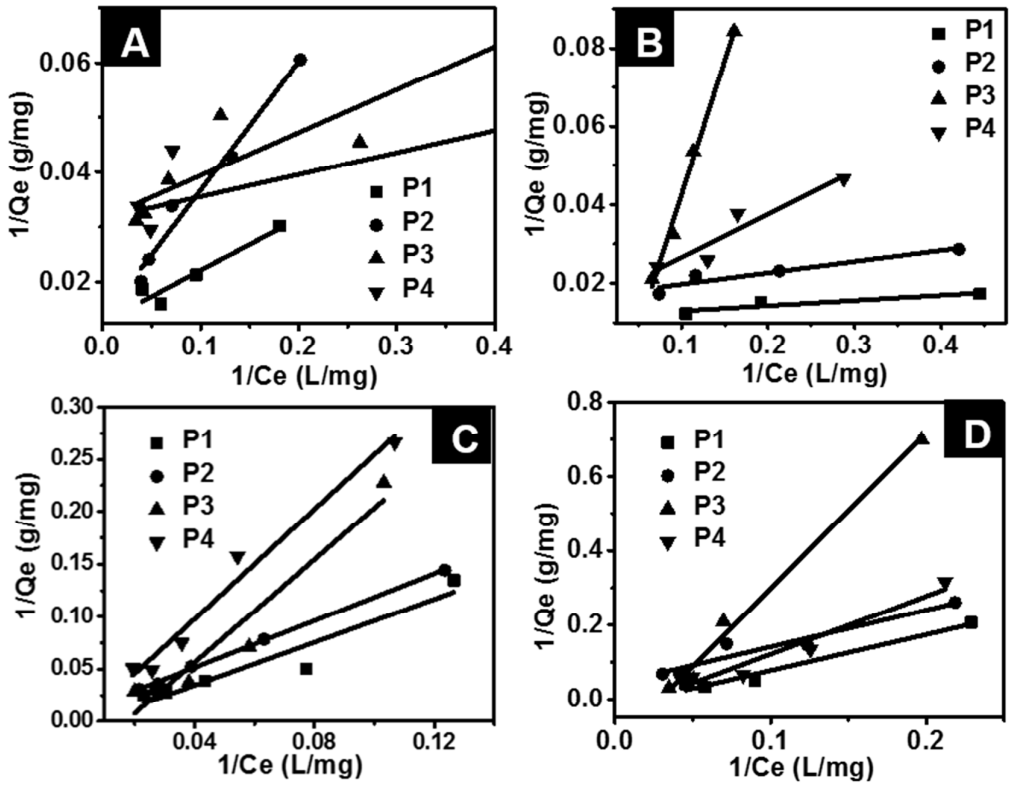

Figure 7. Langmuir isotherm plots for the adsorption of (A) Ag-Cit (B) Ag-PVP (C) Au-Cit and (D) Au-PVP using aminoparticles **P1 - P4**.

Freundlich isotherm model

The extraction data were also analysed using the Freundlich isotherm model, which can be applied for adsorptions on heterogeneous surfaces. The linear plots of these isotherms are shown in Figure 8 and the fitting parameters are summarized in Table 3.

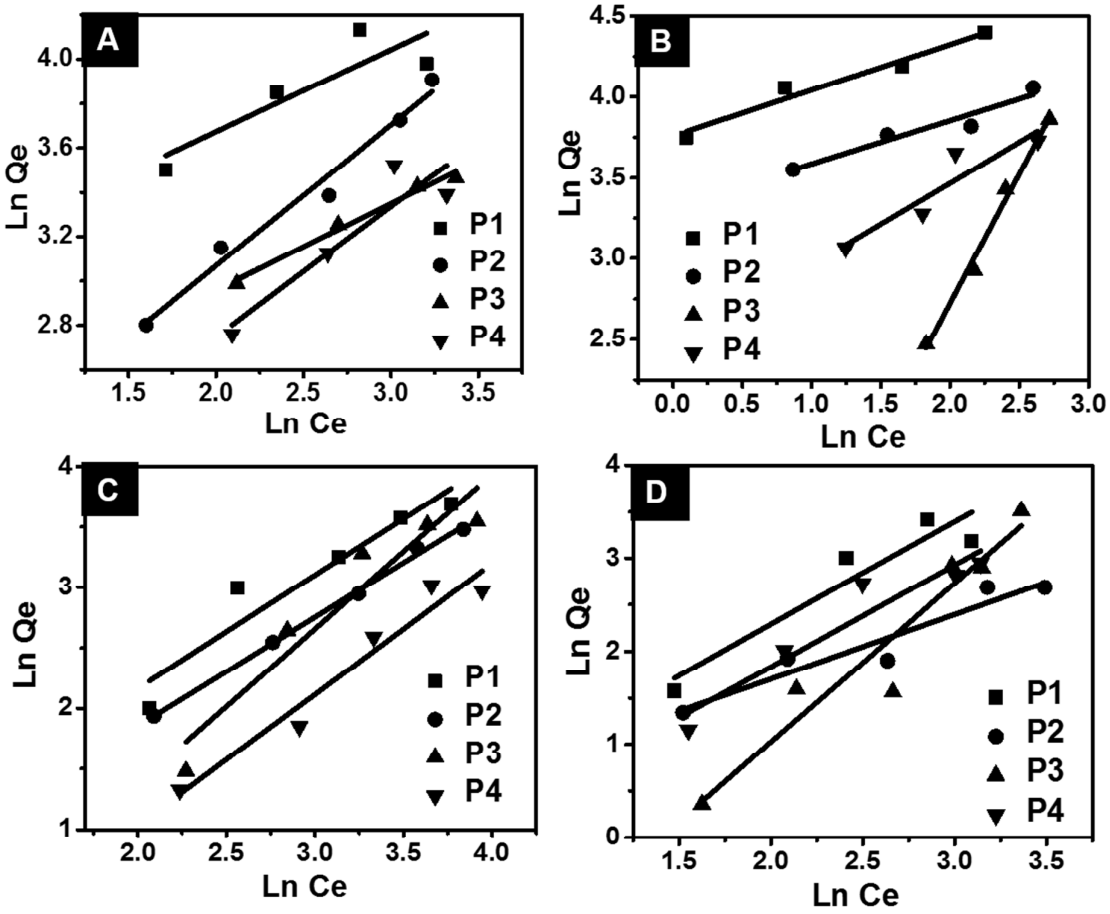

Figure 8. Freundlich isotherm plots for the adsorption of (A) Ag-Cit (B) Ag-PVP (C) Au-Cit and (D) Au-PVP using aminoparticles **P1 - P4**.

The correlation coefficient (R^2) values are lower for the extraction of nanoparticles using all aminoparticles in comparison with the Langmuir model. Also, the $1/n > 1$ values indicate an unfavourable interaction between aminoparticles and NPs.

Interaction between aminoparticle and metal NP interactions

The surface charges on NP's determine the efficiency of adsorption onto the adsorbent surface. Recent studies on the adsorption of metal NP's on various adsorbents have demonstrated both the size and surface charges are critical in determining the efficiency of adsorption.[38-41] A similar trend was observed in our extraction studies with metal NP's. Higher surface charges on the NPs showed better extraction efficiencies owing to electrostatic interactions between the oppositely charged NPs and aminoparticles. The observed low extraction efficiency for neutral PVP-coated NP's as compared to the citrate

capped NPs for the same aminoparticles also highlight the important role played by the electrostatic interaction in extraction process.

Table 3. Langmuir and Freundlich constants for the adsorption of NPs by different aminoparticles

Nano-particles	Amino particles	Langmuir Constants			Freundlich Constants		
		K_L (L g-1)	R_L	R^2	K_f (mg g-1)	1/n	R^2
Ag-Cit	**P1**	0.1329	0.3599	0.91	18.8366	0.3688	0.772
	P2	0.0560	0.5446	0.978	6.0321	0.6357	0.979
	P3	0.4007	0.174	0.93	11.4592	0.3094	0.887
	P4	0.7830	0.1018	0.909	4.8351	0.5868	0.851
Ag-PVP	**P1**	0.9000	0.4476	0.976	42.9527	0.2821	0.965
	P2	0.5813	0.1165	0.909	27.7157	0.2661	0.934
	P3	0.0381	0.6508	0.991	0.6194	1.6019	0.99
	P4	0.1388	0.3477	0.904	11.6069	0.5079	0.863
Au-Cit	**P1**	0.0060	0.8522	0.915	0.5311	1.2200	0.933
	P2	0.0060	0.8296	0.999	1.0607	0.8983	0.997
	P3	0.1690	0.6559	0.935	0.3063	1.2790	0.916
	P4	0.0020	0.9347	0.976	0.3253	1.0796	0.952
Au-PVP	**P1**	0.0224	0.7153	0.969	1.0939	1.1011	0.894
	P2	0.0423	0.5824	0.925	1.3826	0.6905	0.915
	P3	0.0289	0.6648	0.991	0.0926	1.7032	0.921
	P4	0.0220	0.7178	0.948	0.9564	1.0900	0.913

Extraction of metal ions

The extraction of metal ions in aqueous solutions were studied using Pb(II) and Cr(VI) ions. The interactions between the surface amine groups and metal ions in water are used for the removal of contaminants. A steady state was reached within an hour as seen by the plots of extraction efficiency with time (Figure 9).

This is expected owing to the fact that the polymer particles are incorporated with large number of amine groups on the surface. The highest Q_e values for the adsorption of Cr(VI) and Pb(II) are 26.8 mg/g and 93.0 mg/g, respectively, by **P2**, which is closer to Q_e values of **P1** (Table 3). Other amine functionalized aminoparticles showed low extraction efficiencies due to low amine content (Table 1).

Adsorption kinetics

The extraction of metal ions from water is facilitated by the formation of metal-amine complexes. The extraction rate is high during the initial stages owing to easily accessible functional groups for coordination but becomes slower with time, especially after steady-state is reached and the outer surface of the adsorbent is saturated.

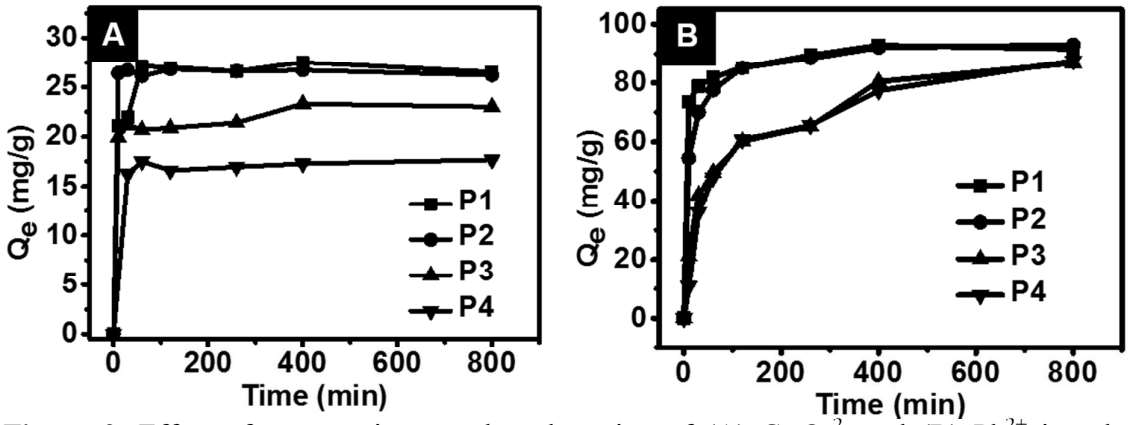

Figure 9. Effect of contact time on the adsorption of (A) $Cr_2O_7^{2-}$ and (B) Pb^{2+} ions by aminoparticles **P1 – P4**.

The extraction kinetics were assessed by employing kinetic models which provide information on the mechanism. It is significant to determine the rate at which the adsorption is achieved when a metal ion is extracted by an adsorbent. The adsorption mechanism includes (a) the diffusion process through which the metal ions diffuse close to the adsorbent surface (b) the chemisorption process and (c) the intra-particle diffusion process.[42]

Among the two widely used kinetic models namely, pseudo-first order and pseudo-second order model, we used the second order kinetics equations to evaluate the extraction process. As shown in Figure 10, the plots of *t/Qt versus t* correspond to linear graphs with correlation coefficients closer to unity (>0.98) for all four aminoparticles and follow pseudo-second order kinetics with respect to the adsorption of Pb(II) and Cr(VI) ions. The calculated Qe values showed good agreement with the experimentally determined numbers. The adsorption of Pb(II) shows extraction efficiencies of 92.8 mg/g, 93.0 mg/g, 86.7 mg/g and 97.5 mg/g for **P1 – P4** and the values are higher than those observed for Cr(VI) ions. The values of the pseudo-second order rate constant, K_2 for all four aminoparticles are summarized in Table 4.

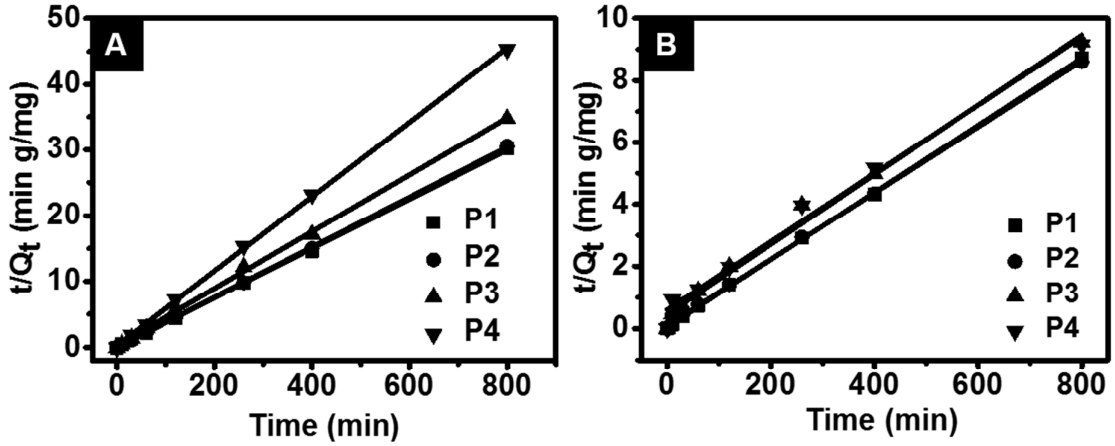

Figure 10. Pseudo-second order kinetics for the extraction of (A) chromium and (B) lead ions using aminoparticles **P1 – P4**

The second order kinetic model assumes that the rate-limiting step involves the chemical interaction between the adsorbent and metal ions leading to a bonding as strong as the covalent bonding.[43] As the extractions follow pseudo-second order, suggesting that the extraction process is very fast with the rate limiting step in our studies is the chemisorption through the interaction of electron rich N and O groups on the surface of adsorbents and electron deficient metal ions in aqueous solution.[44]

Table 4. Pseudo-second order constants and correlation coefficients for the adsorption of Pb(II) and Cr(VI) by aminoparticles **P1 – P4**

Metal ions	**Aminoparticles**	**Q_e (exp) (mg/g)**	**Pseudo-second order kinetic model**		
			Q_e (mg/g)	**K_2 (g/mg min)**	**R^2**
Chromium	**P1**	27.50	26.70	0.12903	0.999
	P2	26.80	26.26	-0.02917	0.999
	P3	23.30	23.12	0.00746	0.999
	P4	17.68	17.67	0.01287	0.999
Lead	**P1**	92.80	92.34	0.00231	0.999
	P2	93.00	93.81	0.00118	0.999
	P3	86.70	88.89	0.00028	0.988
	P4	87.50	90.91	0.00020	0.986

Isotherm studies with chromium and lead ions

Figure 11 shows the Langmuir and Freundlich isotherm plots for the extraction of chromium and lead ions with four aminoparticles and the fitting parameters from these isotherms are summarized in Table 5. On the basis of correlation coefficient (R^2) values for the extraction of chromium ions, the Langmuir model gave values of > 0.98 for **P1**, **P3** and **P4** which are higher than those derived from Freundlich model, thus demonstrating that the extraction of chromium is better explained by this model. In case of lead, the R^2 values for both models are comparable.

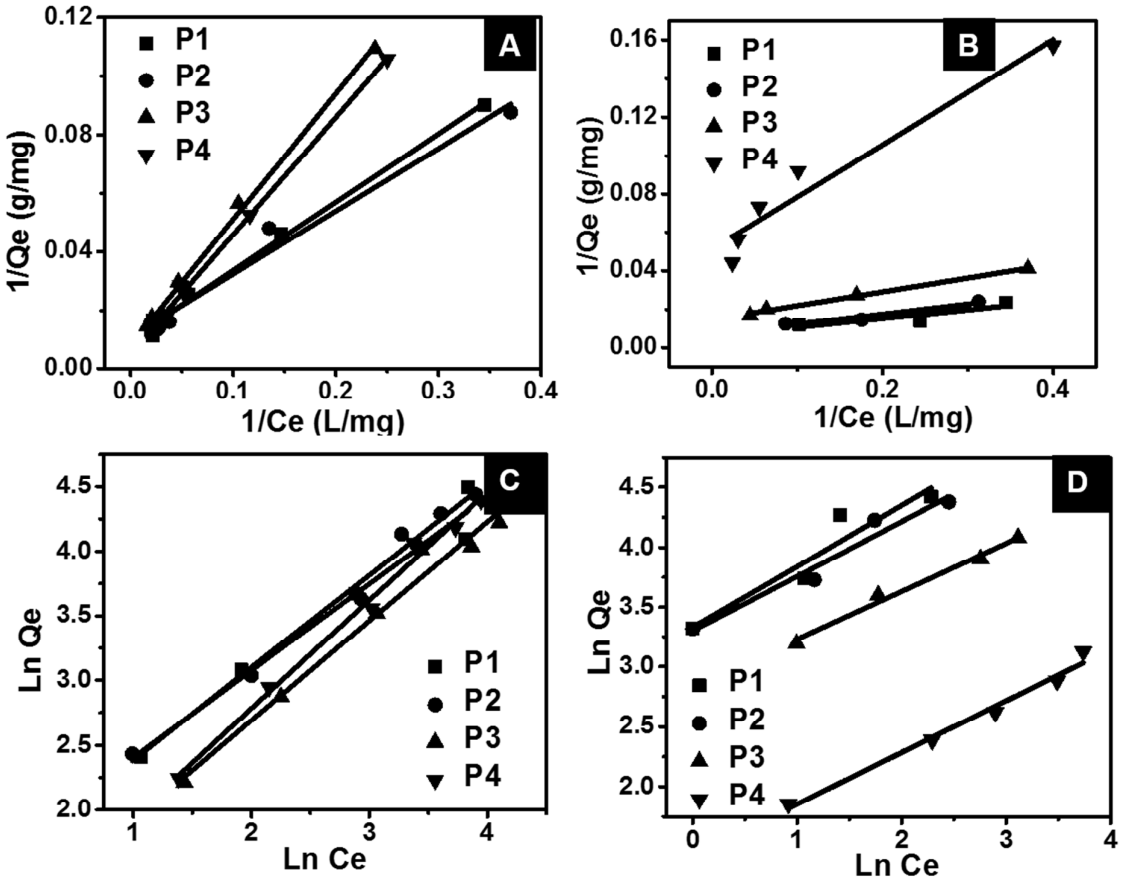

Figure 11. Langmuir (A and B) and Freundlich isotherm (C and D) plots for chromium (A and C) and Lead (B and D) ions.

Based on Langmuir model, the maximum adsorption capacities of Pb^{2+} on the surface of **P1**, **P2** and **P3** is calculated to be 98.0, 84.0 and 67.5 mg/g, respectively. The higher values of the intercept, K_f, for the Pb(II) cation adsorption implies higher extraction capacities.[45] In addition, the equilibrium factor (R_L) is between 0 and 1 for both metal ions suggesting that the adsorption is favourable with all four aminoparticles.

Table 5. Langmuir and Freundlich constants for the adsorption of chromium and lead ions by aminoparticles **P1 - P4**

Metal ions	Aminoparticles	Langmuir Constants			Freundlich Constants		
		K_L (L g^{-1})	R_L	R^2	K_f (mg g^{-1})	1/n	R^2
Chromium	**P1**	0.0301	0.4410	0.981	2.0289	0.9987	0.902
	P2	0.0502	0.3380	0.973	5.3021	0.7157	0.987
	P3	0.0186	0.5450	0.996	3.1667	0.7689	0.980
	P4	0.0139	0.6070	0.997	3.0277	0.8374	0.992
Lead	**P1**	0.3792	0.1942	0.927	27.9440	0.5099	0.907
	P2	0.4722	0.1673	0.932	27.1072	0.4575	0.958
	P3	0.2067	0.7098	0.994	16.8727	0.4027	0.988
	P4	0.1879	0.7263	0.945	4.1632	0.4295	0.985

In the Freundlich model, the 1/n values were all below 1 suggesting heterogeneous binding sites and also chemisorption on the surfaces.[46] The overall results suggest that the extraction of metal ions by the amine functionalized polymer particles is favourable and effective.

Conclusions

Polymer microspheres within the size range of 3 - 5 μm were prepared using copolymerisation of glycidyl methacrylate and styrene using a batch dispersion polymerisation method. These microspheres were subsequently grafted with four different diamines. The aminoparticles obtained were used for the extraction of gold and silver nanoparticles as well as heavy metals such as Pb(II) and Cr(VI) ions from aqueous solutions. Ethylenediamine substituted aminoparticles with high degree of amine loading were found to be efficient adsorbent with an extraction capacities of 91.27, 34.97, 110.88 and 32.11 mg/g for Ag-Cit, Ag-PVP, Au-Cit and Au-PVP, respectively. Both **P1** and **P2** showed highest adsorption towards Pb(II) and Cr(VI) ions, with extraction capacities close to 27 and 93 mg/g, respectively. All extraction experiments with metal nanoparticles and metal ions followed pseudo-second order reaction kinetics, with the correlation coefficients closer to unity and the extractions followed the general order **P1** > **P2** > **P3** > **P4**, proving that the adsorption capacities are proportionate to the amine loading on the adsorbent.

Acknowledgements

The authors thank the National University of Singapore (FRC tier 1 grant) and Environment and Water Industry Programme Office (EWI) under the National Research Foundation of Singapore (PUBPP 21100/36/2, NUS WBS R-706-002-013-290, R-143-000-458-750, R-143-000-458-731) for the financial support of the work. RD also thanks the National University of Singapore for a scholarship for graduate studies.

References

(1) O. Boussif, F. Lezoualc'h, M. A. Zanta, M. D. Mergny, D. Scherman, B. Demeneix, and J. P. Behr, *PNAS*, 1995, **92**, 7297-7301.

(2) C. Volcke, R. P. Gandhiraman, V. Gubala, J. Raj, T. Cummins, G. Fonder, R. I. Nooney, Z. Mekhalif, G. Herzog, S. Daniels, D. W. M. Arrigan, A. A. Cafolla and D. E. Williams, *Biosens. Bioelectron.,* 2010, **25**, 1875-1880.

(3) L. Tauhardt, M. Frant, D. Pretzel, M. Hartlieb, C. Bucher, G. Hildebrand, B. Schroter, C. Weber, K. Kempe, M. Gottschaldt, K. Liefeith and U. S. Schubert, *J. Mater. Chem. B*, 2014, **2**, 4883-4893.

(4) J. B. Sund, C. P. Causey, S. D. Wolter, C. B. Parker, B. R. Stoner, E. J. Toone and J. T. Glass, *Appl. Surf. Sci.*, 2014, **301**, 293-299.

(5) J. M. Goddard and J. H. Hotchkiss, *Prog. Polym. Sci.*, 2007, **32**, 698-725.

(6) C. Boucher, J.-C. Ruiz, M. Thibault, M. D. Buschmann, M. R. Wertheimer, M. Jolicoeur, Y. Durocher and G. De Crescenzo, *Biomaterials*, 2010, **31**, 7021-7031.

(7) E. E. Bedford, S. Boujday, V. Humblot, F. X. Gu and C. M. Pradier, *Colloids Surf., B*, 2014, **116**, 489-496.

(8) Y. Wang, Y. Ke, L. Ren, G. Wu, X. Chen and Q. J. Zhao, *Biomed. Mater. Res. A*, 2009, **88**, 616-627.

(9) L. Dai, H. A. W. Stjohn, J. Bi and P. Zientek, *Surf. Interface Anal.*, 2000, **29**, 46-55.

(10) R. Farley and B. R. Saunders, *Polymer*, 2014, **55**, 471-480.

(11) S. Thaiboonrod, C. Berkland, A. H. Milani, R. Ulijin and B. R. Saunders, *Soft Matter*, 2013, **9**, 3920-3930.

(12) B. Yu, X. Jiang and J. Yin, *Soft Matter*, 2011, **7**, 6853-6862.

(13) J. R. Tauro and R. A. Gemeinhart, *J. Biomater. Sci., Polym. Ed.*, 2005, **16**, 1233-1244.

(14) J. S. Oh, L. N. Dang, S. W. Yoon, P. C. Lee, D. O. Kim, K. J. Kim and J. D. Nam, *Macromol. Rapid Commun.*, 2013, **34**, 504-510.

(15) W.-C. Kuan, D. Horak, Z. Plichta and W.-C. Lee, *Mater. Sci. Eng., C*, 2014, **34**, 193-200.

(16) F. Rui, X. Ge, Z. Li, C. Yang, B. Fang and Y. Liang, *Colloid Polym Sci.*, 2014, **292**, 985-990.

(17) F. Kartal and A. Denizli, *J. Sep. Sci.*, 2014, **37**, 2077-2086.

(18) Z. Yu, R. Wu, M. Wu, L. Zhao, R. Li and H. Zou, *Colloids Surf., B*, 2010, **78**, 222-228.

(19) X. Sun, L. Yang, H. Xing, J. Zhao, X. Li, Y. Huang and H. Liu, *Colloids Surf., A*, 2014, **457**, 160-168.

(20) P. Wu, J.-z. Li, Y.-L. Wang, X.-s. Liu, C. Du, Q.-y. Tong and N. Li, *Biochem. Eng. J.*, 2014, **91**, 66-71.

(21) H. Lu, K. Chandran and D. Stensel, *Water Res.*, 2014, **64**, 237-254.

(22) A. S. Dharnaik and P. K. Ghosh, *Environ. Technol.*, 2014, **35**, 2272-2279.

(23) R. B. Garcia-Reyes and J. R. Rangel-Mendez, *Bioresour. Technol.*, 2010, **101**, 8099-8108.

(24) Y.-S. Yun, D. Park, J. M. Park and B. Volesky, *Environ. Sci. Technol.*, 2001, **35**, 4353-4358.

(25) Z. Li, J. Tang and J. Pan, *Food Control*, 2004, **15**, 565-570.

(26) P. V. AshaRani, G. K. M. Low, M. P. Hande and S. Valiyaveettil, *ACS Nano*, 2009, **3**, 279-290.

(27) S. Dalai, S. Pakrashi, M. Joyce Nirmala, A. Chaudhri, N. Chandrasekaran, A. B. Mandal and A. Mukherjee, *Aquat. Toxicol.*, 2013, **138–139**, 1-11.

(28) E.-J. Park, J. Yi, Y. Kim, K. Choi and K. Park, *Toxicol. in Vitro*, 2010, **24**, 872-878.

(29) J. Polte, R. Erler, A. F. Thünemann, S. Sokolov, T. T. Ahner, K. Rademann, F. Emmerling and R. Kraehnert, *ACS Nano*, 2010, **4**, 1076-1082.

(30) D. L. Van Hyning, W. G. Klemperer and C. F. Zukoski, *Langmuir*, 2001, **17**, 3128-3135.

(31) M. Ma, Q. Zhang, Y. Liu, H. Zhang, W. Wang, Y. Chen and J. Gu, *J. Dispersion Sci. Technol.*, 2012, **33**, 1173-1178.

(32) X. Sun, L. Yang, H. Xing, J. Zhao, X. Li, Y. Huang and H. Liu, *Chem. Eng J.*, 2013, **234**, 338-345.

(33) A. M. Donia, A. A. Atia and F. I. Abouzayed, *Chem. Eng J.*, 2012, **191**, 22-30.

(34) R. Mallampati and S. Valiyaveettil, *ACS Appl. Mater. Interfaces*, 2013, **5**, 4443-4449.

(35) N. Mahanta, W. Y. Leong and S. Valiyaveettil, *J. Mater. Chem.*, 2012, **22**, 1985-1993.

(36) N. Mahanta and S. Valiyaveettil, *Nanoscale*, 2011, **3**, 4625-4631.

(37) R. Mallampati and S. Valiyaveettil, *RSC Adv.*, 2012, **2**, 9914-9920.

(38) W.-C. Hou, B. Y. Moghadam, C. Corredor, P. Westerhoff and J. D. Posner, *Environ. Sci. Technol.*, 2012, **46**, 1869-1876.

(39) W.-C. Hou, B. Y. Moghadam, P. Westerhoff and J. D. Posner, *Langmuir,* 2011, 27, 11899–11905.

(40) T. Brenner, M. Paulus, M.A. Schroer, S. Tiemeyer, C. Sternemann, J. Möller, M. Tolan, P. Degen and H. Rehage, *Journal of Colloid and Interface Science*, 2012**, 374**, 287-290.

(41) P. Wagener, A. Schwenke and S. Barcikowski, *Langmuir*, 2012**, 28**, 6132-6140.

(42) G. Barassi, A. Valdés, C. Araneda, C. Basualto, J. Sapag, C. Tapia and F. Valenzuela, *J. Hazard. Mater.*, 2009, **172**, 262-268.

(43) P. Ding, K.-L. Huang, G.-Y. Li and W.-W. Zeng, *J. Hazard. Mater.*, 2007, **146**, 58-64.

(44) Y. S. Ho and G. McKay, *Water Res.*, 2000, **34**, 735-742.

(45) X. Guo, B. Du, Q. Wei, J. Yang, L. Hu, L. Yan and W. Xu, *J. Hazard. Mater.*, 2014, **278**, 211-220.

(46) J.-Q. Jiang, C. Cooper and S. Ouki, *Chemosphere*, **2002**, 47, 711-716.